energies

MDPI

Article

Analytical and Experimental Study of Thermoelectric Generator (TEG) System for Automotive Exhaust Waste Heat Recovery

Faisal Albatati * and Alaa Attar

Department of Mechanical Engineering, Faculty of Engineering at Rabigh, King Abdulaziz University, Jeddah 21589, Saudi Arabia; Loattar@kau.edu.sa
* Correspondence: alalbatati@kau.edu.sa

Abstract: Nearly 70% of the energy produced from automotive engines is released to the atmosphere in the form of waste energy. The recovery of this energy represents a vital challenge to engine designers primarily when a thermoelectric generator (TEG) is used, where the availability of a continuous, steady-state temperature and heat flow is essential. The potential of semi-truck engines presents an attractive application as many coaches and trucks are roaming motorways at steady-state conditions most of the time. This study presents an analytical thermal design and an experimental validation of the TEG system for waste heat recovery from the exhaust of semi-truck engines. The TEG system parameters were optimized to achieve the maximum power output. Experimental work was conducted on a specially constructed setup to validate the analytically obtained results. Both analytical and experimental results were found to be in good agreement with a marginal deviation, indicating the excellent accuracy of the effective material properties applied to the system since they take into account the discrepancy associated with the neglection of the contact resistances and Thomson effect.

Keywords: thermal design of thermoelectric system; energy balance of thermoelectric generator; waste heat recovery system

Citation: Albatati, F.; Attar, A. Analytical and Experimental Study of Thermoelectric Generator (TEG) System for Automotive Exhaust Waste Heat Recovery. *Energies* **2021**, *14*, 204. https://doi.org/10.3390/en14010204

Received: 27 November 2020
Accepted: 27 December 2020
Published: 2 January 2021

1. Introduction

Generally, it is estimated that about one third of total energy is usefully used while the remaining two thirds are rejected as waste heat. In the automotive industry, particularly, the internal combustion engine has a maximum efficiency of nearly 25%, while the remaining 75% of energy is lost in the form of waste heat from exhaust gases and engine coolant [1]. Many studies have investigated the recovery of waste heat from internal combustion engines using different technologies. Thermoelectric technology is seen as one of the most promising technologies to exploit this waste heat. This is mainly due to the continuous advancement of the materials used in manufacturing thermoelectric modules and, therefore, their overall efficiency [2]. The technology itself is based on a unique solid-state power device that can be easily used in vehicle exhaust pipes to recover a portion of the waste heat and convert it into useful electricity.

The earliest experimental attempt on a thermoelectric exhaust generator system for an automotive was conducted by Neild in 1963, as reported by Fagehi et al. [3]. The study's main target was to produce 500 W of power at 28 V with a minimum efficiency of 3%. The results showed that the maximum power output and efficiency achieved were 156.6 W and 2.2%, respectively. In 1988, Porsche developed a prototype to test a thermoelectric generator (TEG) using the exhaust gas and water circulation systems. The thermoelectric material used was iron silicide ($FeSi_2$), which was connected to the Porsche 944 engine. The temperature difference between the cold and the hot sides of thermoelements was 490 K, and the achieved power output was 58 W for 90 thermoelements [4]. In 1994, Bass, Elsner, and Leavitt [5] developed a thermoelectric power generator system for diesel truck engines with a target power output of 1 kW. The system used 72 thermoelectric modules

and achieved a maximum power output of 1068 W at 300 HP and 1700 RPM. The study also reported that bismuth telluride (Bi_2Te_3) was the best thermoelectric material for exhaust waste heat applications, as it demonstrated the highest performance despite the maximum operating temperature.

Matsubara [6] developed a high-efficiency TEG for gasoline engines in 2002. The TEG prototype was installed in a pick-up truck, and a 1–2% improvement in fuel efficiency was reported depending on the truck's speed. The study concluded that average ZT-values from 1.5 to 2 were needed in order to achieve 10% overall efficiency. Researchers at BMW developed a Bi_2Te_3 TEG prototype in 2009. The TEG consisted of 24 modules and achieved 200 W of electrical power output at a speed of 130 km/h [7]. Simultaneously, General Motors developed a TEG system with an anticipated power output of 350 W and 600 W under city and highway driving conditions, respectively [8]. The tested thermoelectric module achieved a maximum power output of 9 W at constant hot and cold junction temperatures of 550 °C and 80 °C, respectively [9].

Yu and Chau [10] theoretically investigated a TEG system for automotive exhaust, and then experimentally analyzed the maximum power output. Their study also investigated the relationship between power output and load resistance at various hot-side temperatures. The results indicated that as the temperature of the hot side increased, the internal load resistance would also increase.

Liu et al. [11] constructed a TEG energy-harvesting system for automotive exhaust pipes. The system was practically tested on-road, achieving an efficiency of 1.25% and a maximum power output of 600 W at an average temperature difference of 182 °C. The study concluded that design optimization was essential for improving the system's performance.

To improve the TEG module performance, Zhang et al. [12] developed a nanostructured bulk material and manufactured module that has a power density of 5.26 W/cm^2 and a temperature difference of 500 °C. The authors designed and constructed a TEG system that consisted of 400 modules, and tested it on an automotive diesel engine. The maximum produced power output was 1002.6 W, at an average temperature of 550 °C and an exhaust mass flow rate of 480 g/s.

Kim et al. [13] experimentally investigated a TEG system for waste heat recovery of a six-cylinder diesel engine. The system included 40 customized modules installed on a rectangular heat exchanger with a dimension of 253.5 mm × 372 mm × 60 mm. The engine was operated with a rotational speed in the range of 1000–2000 RPM, and an engine brake mean effective pressure of 0.2–1.0 MPa. The maximum power output achieved was 119 W at 2000 RPM and 0.6 MPa, while the conversion efficiency was in the range of 0.9–2.8%. The study indicated that the power output increased with the engine load or speed, and the pressure drops were below 1.46 kPa under all experimental conditions.

In their study on automotive exhaust thermoelectric generators, Li et al. [14] investigated the influence that the number of thermoelectric modules and their distribution patterns had on the system performance. The system consisted of Bi_2Te_3-based modules and was installed on a 11.12 L automotive diesel engine. The independent cooling system consisted of 18 single-column water tanks. The results showed that the best results were achieved when the exhaust temperature and mass flow rate were 805 K and 0.5 kg/s, respectively. The maximum electrical power generated was 217.35 W, and the conversion efficiency was 3.45%.

In a recent innovative study, Li et al. [15] designed and tested a mesoscale combustor-powered TEG with enhanced heat collection. The system absorbed heat from a stagnation-point reverse-flow (SPRF) combustor, and was also equipped with a built-in heat exchanger that rejects heat to a water-cooled heat sink. Among the several methods investigated to improve both power output and thermoelectric efficiency, the study indicated that the load resistance ratio must be greater than one; however, the study did not determine this value.

From previous studies in the open literature regarding TEG systems for automotive exhaust, it is apparent that their main limitations are their very low densities of waste heat and their improper design despite the system's size. The current study presents an analyti-

cal design and experimental validation for a TEG system that captures waste heat from the exhaust of semi-trucks' engines which travel for long distances between destinations, subsequently providing continuous waste heat exhaust gas at constant temperatures and steady flow rates. The proposed design focuses on maximizing the electrical power output from the TEG system by optimizing the electrical load resistance as well as the number of thermoelements of the TEG module. The TEG system is an air-to-liquid system, where the cooling liquid is extracted from the cooling system of the engine in order to absorb the heat from the cold side of the TEG. To maximize the exploitation of the exhaust gas, a heat sink is used, with parameters such as fin thickness and fin spacing optimized using a classical analytical model. A unit cell of the TEG system was modelled, and then the results were extrapolated to determine the results for the whole system. The key contribution of this work is that the governing equation of the model was formulated using six equations where the enthalpy flow equation for the hot gases and cooling fluid were used to determine the fluid outlet temperatures. These temperatures were considered to be the unknown variables in addition to the other typical TEG junction temperatures. Furthermore, the analytically obtained results were validated using a specially constructed experimental setup, where the primary contribution here is to allow simple determination of the TEG module junction temperatures from the measured hot and cold fluid outlet temperatures, as will be explained the following sections.

2. Analytical Design

2.1. Automotive Exhaust TEG System

The proposed automotive exhaust TEG system consists of four main components, as illustrated in Figure 1. These components are: the thermoelectric (TE) modules that convert the waste heat into electricity, a heat sink that captures the heat from the flowing exhaust gas and transfers it to the hot side of the modules, and a heat exchanger that dissipates the heat from the cold side of the modules. The location of the TEG system in the exhaust pipe is crucial to the system's performance, where it has to be ideally located as close as possible to the catalytic converter to allow maximum exploitation of the steady heat emitted [16].

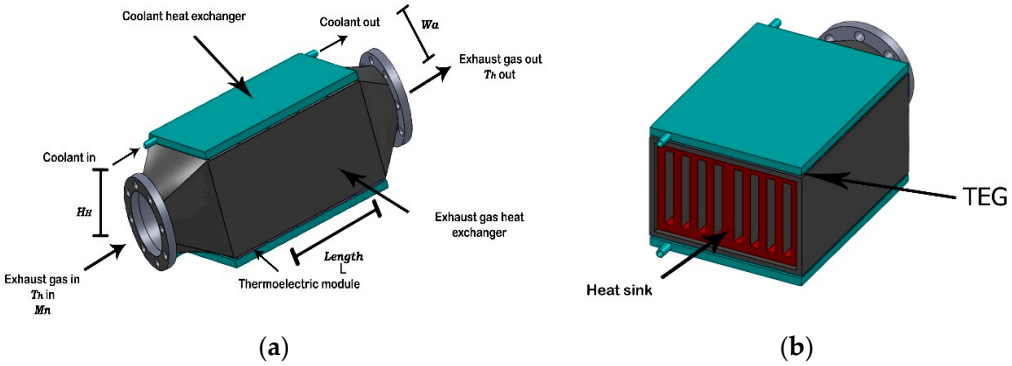

Figure 1. Three-dimensional model of the proposed system: (**a**) thermoelectric generator (TEG) whole system; (**b**) cutaway view of the proposed system.

2.2. Thermoelectric Unit Cell Design

To simplify the proposed model, the system was divided into TEG system unit cells. The design of the TEG cell was modelled analytically by six governing Equations (1)–(6). Figure 2 shows the thermoelectric module placed between the heat exchanger (the hot side) and the heat sink (the cold side).

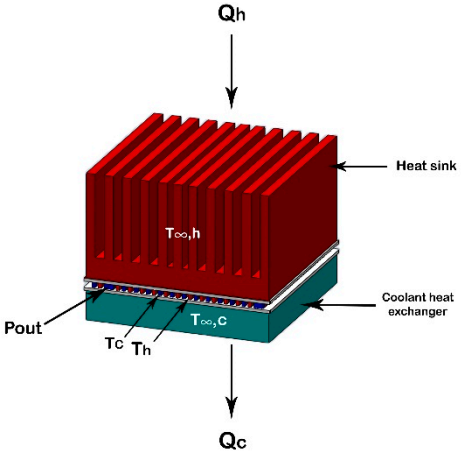

Figure 2. The thermoelectric unit cell of the proposed design.

The governing equations of the system were formulated under the following assumptions:

- The steady-state heat flow is at a constant rate.
- The TEG module contact resistances are neglected.
- The Thomson effect (which is the temperature-dependent material properties) is neglected.
- The heat transfer that takes place by convection and radiation through the TEG module is neglected.

The six governing equations are as follows:

$$\dot{Q}_h = \dot{m}_h Cp_{gas}(T_{h.in} - T_{h.out}) \tag{1}$$

$$\dot{Q}_h = \eta_h h_h A_h \left[\frac{(T_{h.in} + T_{h.out})}{2} - T_h \right] \tag{2}$$

$$\dot{Q}_h = n \left[\alpha \frac{\alpha(T_h - T_c)}{\frac{R_L}{n} + R_e} T_h - \frac{1}{2} \left[\frac{\alpha(T_h - T_c)}{\frac{R_L}{n} + R_e} \right]^2 R_e + K_e(T_h - T_c) \right] \tag{3}$$

$$\dot{Q}_c = n \left[\alpha \frac{\alpha(T_h - T_c)}{\frac{R_L}{n} + R_e} T_c + \frac{1}{2} \left[\frac{\alpha(T_h - T_c)}{\frac{R_L}{n} + R_e} \right]^2 R_e + K_e(T_h - T_c) \right] \tag{4}$$

$$\dot{Q}_c = h_c A_c \left[T_c - \frac{(T_{c.in} + T_{c.out})}{2} \right] \tag{5}$$

$$\dot{Q}_c = \dot{m}_c Cp_{coolant}(T_{c.out} - T_{c.in}) \tag{6}$$

$\dot{Q}_h$ is the heat input into the system, and $\dot{Q}_c$ is the heat rejected from the system in Watts. $\dot{m}_h$ and $\dot{m}_c$ are the mass flow rate of the exhaust gas and the cooling water in kg/s, respectively. Cp is the specific heat of either exhaust gas or for coolant in kJ/kg·K. $T_{c.in}$ and $T_{c.out}$ are the coolant water inlet and outlet temperatures in kelvin, and similarly, $T_{h.in}$ and $T_{h.out}$ are the inlet and outlet temperatures for the exhaust gas. T_h *and* T_c are the junction temperatures of the TEG module in kelvin. h is the heat transfer coefficient of either the coolant or the exhaust gas in W/m^2·K. A_h and A_c are the heat transfer areas for the hot-side sink and cold-side heat exchanger, respectively. η_h is the overall heat sink efficiency, and n is the number of thermoelements inside the TEG. K_e is the TEG thermal conductance in W/K obtained from the TEG element geometric ratio and element thermal conductivity. R_e is the TEG module electrical resistance in ohms obtained from the element geometric ratio and the element electrical resistivity. Finally, the six unknown variables from the governing equations are $\dot{Q}_h$, $\dot{Q}_c$, T_h, T_c, $T_{h.out}$, and $T_{c.out}$. It is also important to note that

the electrical current which appears in similar work found in the literature is replaced in the current study by using the term $\frac{\alpha(T_h - T_c)}{\frac{R_L}{n} + R_e}$ in Equations (3) and (4) to present the relationship between the heat input $\dot{Q}_h$ and heat rejection $\dot{Q}_c$ versus the electrical load resistance, as indicated by Lee [17].

Subsequently, the power output can be calculated as:

$$\dot{Q}_h = P_{out} + \dot{Q}_c \tag{7}$$

The efficiency of the TEG module is given by:

$$\eta_{TE} = \frac{P_{out}}{\dot{Q}_h} \tag{8}$$

2.3. Heat Sink

The heat sink's function is to absorb and reject heat into the surrounding air by increasing the heat transfer surface area with fins and spines [18]. This section's main objective is to present the design of a heat sink that can absorb the maximum possible waste heat coming from the exhaust. To do so, the fin thickness t_f and the fin spacing z_f were optimized. Figure 3 illustrates the heat sink and its design parameters.

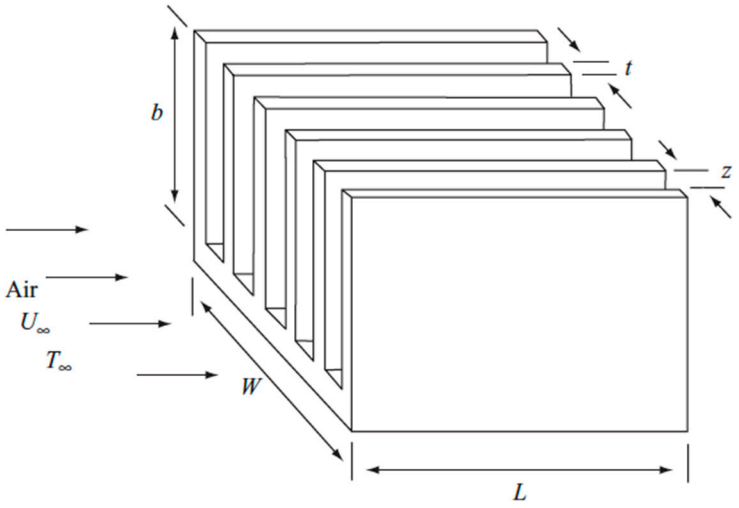

Figure 3. Forced convection multiple fin array.

The overall thermal resistance of the heat sink is given by:

$$R_t = \frac{1}{\eta h A_t} \tag{9}$$

The overall efficiency of the heat sink is:

$$\eta = 1 - n\left(\frac{A_f}{A_t}\right)\left(1 - \eta_f\right) \tag{10}$$

The total area is calculated by:

$$A_t = n\left[2\left(L + t_f\right)b_{HS} + Lz_f\right] \tag{11}$$

Moreover, the single fin area is given by:

$$A_f = 2\left(L + t_f\right)b_{HS} \tag{12}$$

The heat transfer coefficient is given by:

$$h = \frac{N_u K_w}{D_h} \tag{13}$$

The turbulent flow Nusselt number inside a duct is:

$$N_u = \frac{\left(\frac{f}{2}\right)(R_e - 1000)P_r}{1 + 12.7\left(\frac{f}{2}\right)^{0.5}\left(P_r^{2/3} - 1\right)} \tag{14}$$

The Reynold's number is:

$$R_e = \frac{U_w D_h}{v_w} \tag{15}$$

The hydraulic diameter is calculated as:

$$D_h = \frac{4A_{cw}}{2(b_w + w_b)} \tag{16}$$

The friction factor is:

$$f = [1.58\ln(R_e) - 3.28]^{-2} \tag{17}$$

The total volume flow rate total is:

$$V_t = UA \tag{18}$$

where U is the velocity.

The pressure drop is calculated by:

$$\Delta P = \frac{4fL}{D_h}\frac{\rho u^2{}_m}{2} = \frac{2fL}{D_h}\frac{G^2}{\rho} \tag{19}$$

The optimum fin spacing z_f can be calculated as:

$$Z_f = 3.24 Re_L^{-1/2} Pr^{-\frac{1}{4}} L \tag{20}$$

2.4. Effective Material Properties

Most TEG module manufacturers do not provide the thermoelectric material properties. Moreover, the thermoelectric ideal equations (i.e., Equations (3) and (4)) do consider neither the effect of contact resistance nor the Thomson effect. To resolve these shortcomings, the effective material properties presented by Weera et al. [19] were used, where these properties were back-calculated from the manufacturer's maximum parameters. Besides the virtue of directly obtaining the required material properties, this method's advantage is demonstrated in accounting for the errors associated with neglecting the contact resistances and Thomson effects.

The effective thermal conductivity is given by:

$$k^* = \frac{{\alpha^*}^2}{\rho^* z^*} \tag{21}$$

The effective electrical resistivity is given by:

$$\rho^* = \frac{4\left(\frac{A}{L}\right)\dot{W}_{max}}{n(I_{max})^2} \tag{22}$$

The effective Seebeck coefficient is:

$$\alpha^* = \frac{4\dot{W}_{max}}{nI_{max}(T_h - T_c)} \tag{23}$$

The effective figure of merit is:

$$Z^* = \frac{\frac{2}{T_{avg}}\left(1 + \frac{T_c}{T_h}\right)}{\eta_c\left(\frac{1}{\eta_{mp}} + \frac{1}{2}\right) - 2} \tag{24}$$

A/L is the element geometric ratio, η_c, is the Carnot efficiency of the TEG module, η_{mp} is the maximum power efficiency of the TEG module, and T_{avg} is the average temperature between the hot and cold junctions of the TEG module.

3. Experimental Work

3.1. Experimental Procedure

An experimental setup was specially constructed to validate the analytically obtained results. As depicted in the schematic diagram of the experimental setup in Figure 4, a thermoelectric module (TEC1-12706) was attached to an aluminum heat sink 40 mm × 40 mm × 10 mm in dimension, which was placed inside a fabricated aluminum channel 40 mm × 40 mm × 150 mm in dimension. The hot air was supplied to the heat sink through the channel by a heat gun that emulated the exhaust gas. The entire hot-side channel was insulated by high-temperature insulation. An anemometer of ±5% accuracy was used to measure the hot air velocity at the exit of the hot-side channel. A specially fabricated aluminum channel 40 mm × 20 mm × 150 mm in dimension was used as a heat exchanger on the cold side. A small water pump with a known volumetric flow rate circulated cooling water through the cold-side channel. Lastly, the inlet and outlet temperatures of the hot and cold fluids were measured using four K-type thermocouples with standard limits of error of 0.75%, placed at the inlets and the outlets of the channels. Figure 5 shows the different views of the experimental setup.

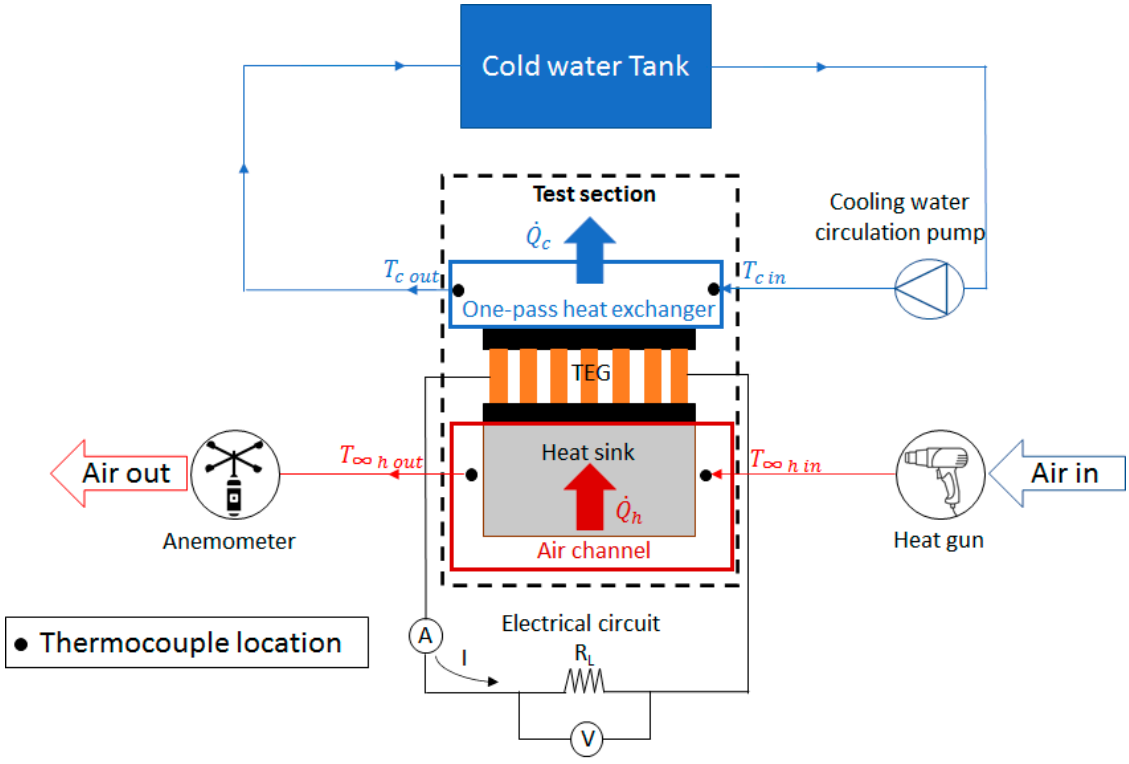

Figure 4. Schematic diagram of the experimental setup.

The hot and cold fluid flow rate, as well as the hot and cold fluid inlet temperatures, were set and kept constant throughout the experiment. The experiment was designed to measure the steady-state inlet and outlet temperatures of the hot and cold fluid, as well as the output current and voltage generated from the TEG module, using two multimeters of ±2% accuracy for different load resistances. The experimental procedure, as well as the logged and measured parameters, are illustrated in the experimental flowchart shown in Figure 6.

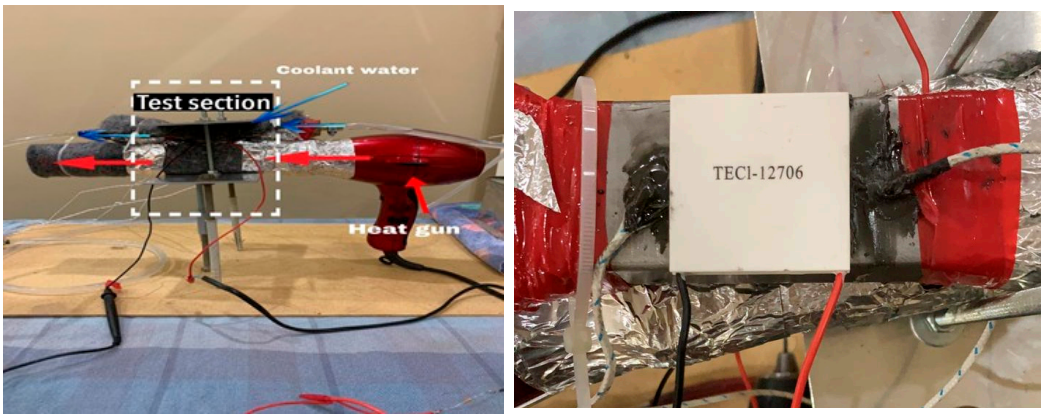

(**a**) (**b**)

Figure 5. Experimental setup: (**a**) overview; (**b**) top view of the test section.

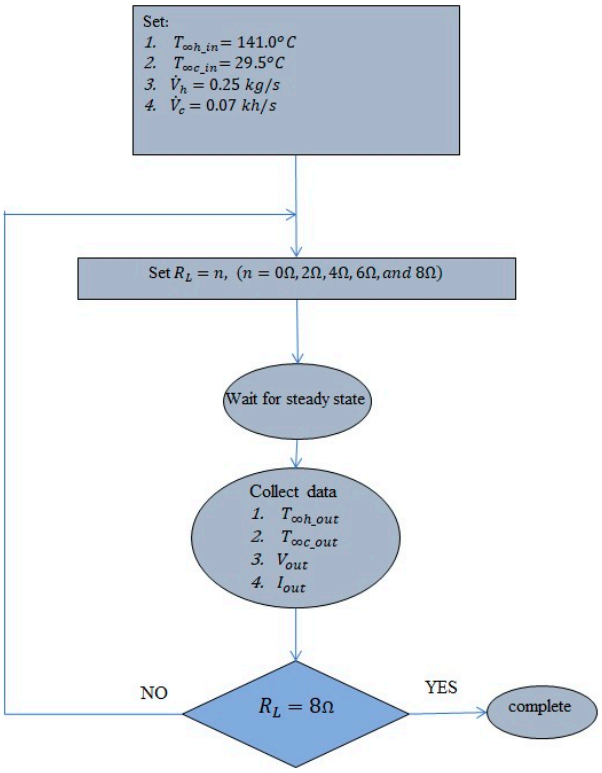

Figure 6. Flow chart of the experimental procedures.

4. Results and Discussion

The analytical model inputs were the semi-truck's engine exhaust gas properties, where the exhaust gas entered the TEG system at a temperature of 550 °C, with a mass flow rate of 0.032 kg/s [2]. At the heat sink, the cooling liquid was ethylene glycol at a

temperature of 90 °C and flow rate of 0.237 kg/s. In order to simplify the approach towards the presented results, the analysis and experimental work were conducted on one TEG unit cell where the hot inlet air and cooling water temperatures were averaged in the middle of the whole system, assuming a linear change of the temperatures along the whole system as proven by Fagehi [2]. After the power output and power density of the unit cell were determined, the result of the whole system was extrapolated using the obtained power density of the unit cell.

4.1. Prediction of Effective Material Properties

To establish the accuracy of the effective material properties as in Equations (21)–(24), a commercial thermoelectric module was tested, with the results of the module performance shown in Table 1 and Figure 7. The results show the relationship between voltage and output power versus hot junction temperature for predicted values using effective material properties and manufacturer's data. A comparison of the predicted results with the manufacturer's data shows an excellent agreement, indicating the validity of the effective material properties approach. The calculated effective material properties are shown in Table 1. Figure 7 shows a comparison between the predicted performance using the effective material properties and the manufacturer's performance.

Table 1. The results of effective material properties for (TMG-127-1.0-0.8) at $T_h = 200$ °C, $T_c = 30$ °C, $n = 127$, $A_e = 1$ mm^2, and $L_e = 1.35$ mm.

Input Parameters (from Manufacturer)			
$V_{max} = 3.0$ V	$I_{max} = 3.0$ A	$W_{max} = 5.1$ W	$\eta_{mp} = 4.8\%$
Effective Material Properties			
$\alpha^* = 314.96 \frac{\mu \cdot V}{K}$	$k^* = 0.03 \frac{W}{cm \cdot K}$	$\rho^* = 2.23 \times 10^{-3}\ \Omega \cdot cm$	$z^* = 1.492 \times 10^{-3} \frac{1}{K}$

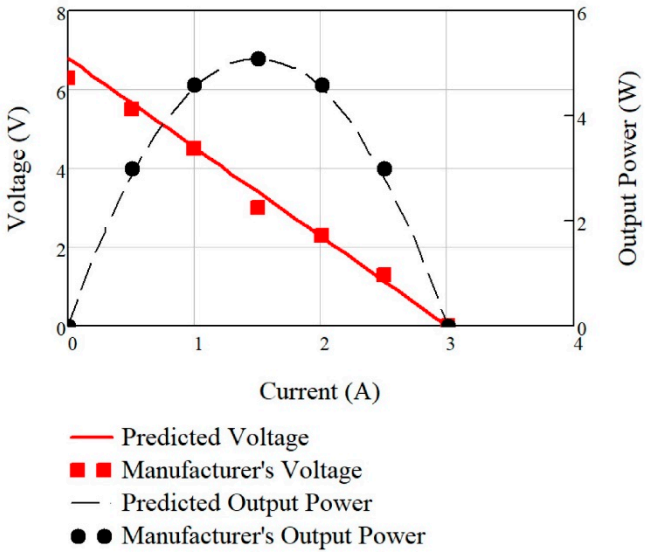

Figure 7. Comparison between the predicted performance using the effective material properties and the manufacturer's performance.

The heat sink's total heat transfer rate was calculated by optimizing the fin thickness using Equations (9)–(19), and was found to be 2 mm, as shown in Figure 8. Moreover, the optimum fin spacing was independently calculated using Equation (20), and was found to be 1.35 mm. The total heat transfer rate at optimum fin spacing and thickness was 166 W. The pressure drop along the whole system had a significant effect on automotive engine performance and fuel consumption, and was found to be 0.27 Pa—well below the limit of 812 Pa indicated by Kumar et al. [20].

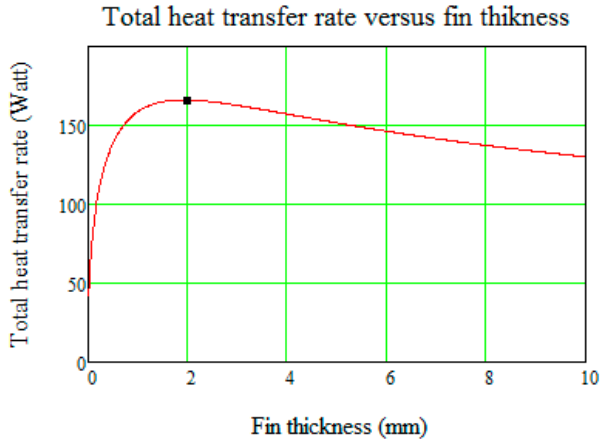

Figure 8. Total heat transfer rate versus fin thickness.

4.2. TEG System Modelling Results

Solving the system's governing Equations (1)–(6) for the six unknown parameters mentioned in Section 2.2 yielded the relationship between power output and load resistance. Figure 9 shows the TEG system's power output and the thermoelectric efficiency variations at different load resistances and different numbers of thermoelements. Simultaneously, the optimum number of thermoelements was obtained, as shown in Figure 10, where the power output and efficiency are plotted for various numbers of thermoelements at different load resistances. Table 2 presents the optimum results for a single TEG cell as well as the whole TEG system, for a semi-truck engine exhaust. As shown, the optimum load resistance for the system was identified as 400 Ω, and the optimum number of thermoelements was 12,700, to produce the maximum electrical power output of 1250 W.

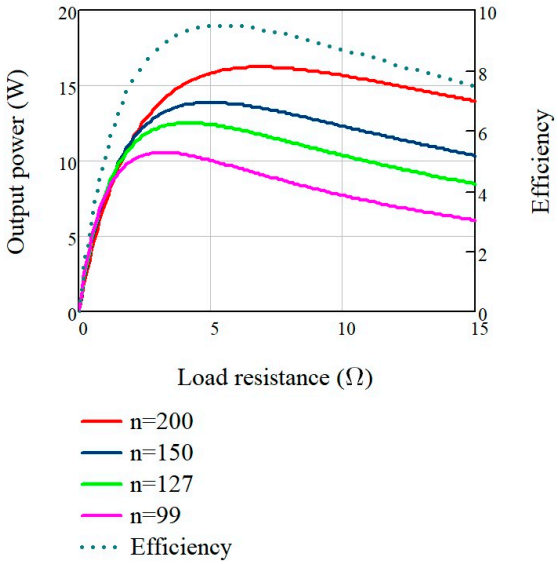

Figure 9. The relationship between load resistance ratio, TEG system power output, and thermoelectric efficiency.

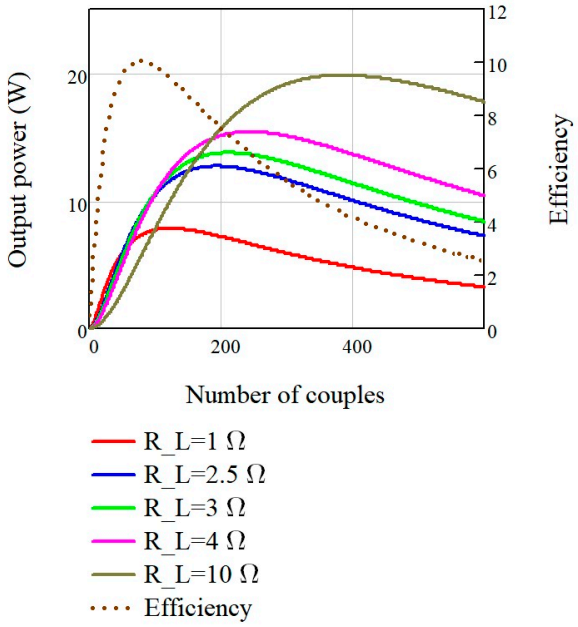

Figure 10. The relationship between the number of thermoelements, TEG system power output, and thermoelectric efficiency.

Table 2. The optimum TEG system parameters of the analytical model.

The optimum Design of a TEG Cell					
R_L (Ω)	n	A (cm^2)	T_h (°C)	T_c (°C)	P_{OUT} (W)
4	127	9	516.47	139.76	12.5
The Optimum Design of the TEG System					
$R_{L.total}$ (Ω)	n_{total}	A_{total} (cm^2)	T_h (°C)	T_c (°C)	$P_{OUT.total}$ (W)
400	12,700	900	516.47	139.76	1250

4.3. Experimental Validation

To validate the analytically modelled system's results, the thermoelectric module TEC1-12706 from Section 3.1 was used to emulate a TEG unit cell of the whole TEG system. Its effective material properties are shown in Table 3. On the experimental setup's hot side, to mimic the exhaust gas, hot air was supplied to the test section by a hot air gun with temperature and mass flow rate maintained at 141 °C and 0.025 kg/s, respectively. As for the cold side, water was used to mimic the ethylene glycol. The cooling water entering the test section was maintained at a temperature of 29.5 °C and a mass flow rate of 0.07 kg/s throughout the test. Furthermore, an analytical model based on the experimental test inputs was carried out purposely to simulate the experiment. Figure 11 shows a comparison between the experiment and the analytical outlet temperatures for the hot and cold fluids at various electrical load resistances. As can be seen, the analytical and the experimental results at the cold side are in good agreement, with an apparent slight discrepancy for the hot side results, which was mainly due to insulation losses. The figure also presents the analytical junction's hot and cold temperatures. A significant change in the cold junction temperature can be seen due to the change in the load resistance, which is verified by several other studies as presented by Attar et al. [21]. Furthermore, a good agreement between the experimentally obtained electrical power output results and the analytically obtained power outputs at variable load resistance is shown in Figure 12. The figure also shows the analyzed errors where the maximum noted error of the output power was 4%.

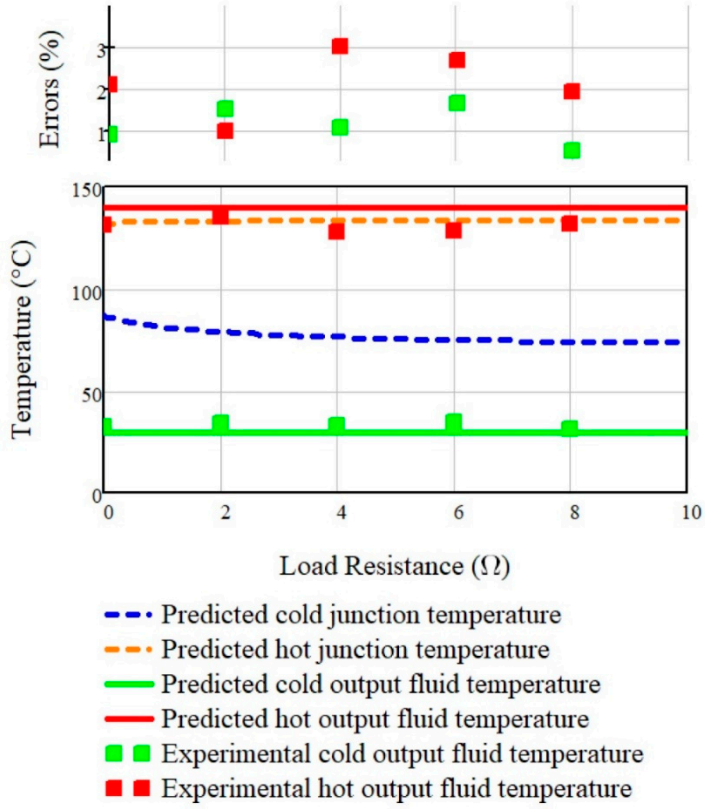

Figure 11. The relation between temperatures and the error associated with outlet temperatures and load resistance.

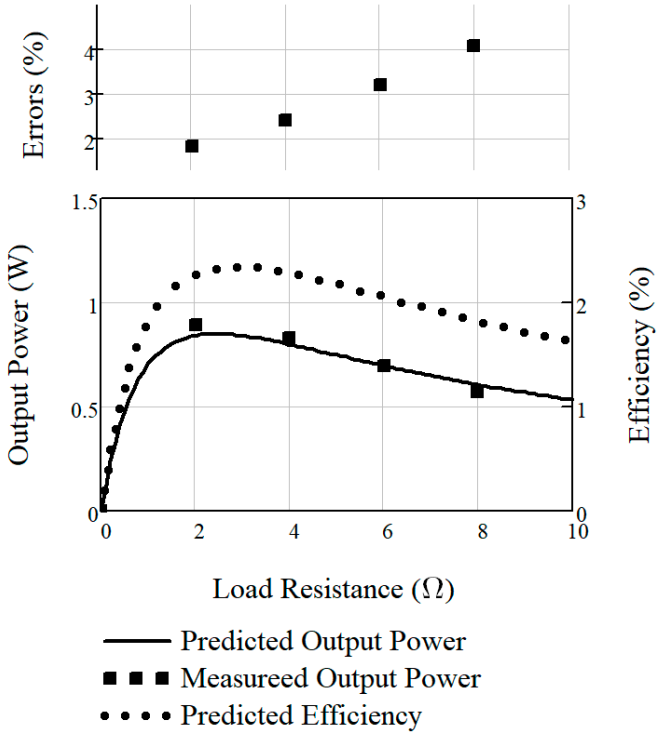

Figure 12. The relation between output power and its associated error and efficiency versus load resistance.

Table 3. Experimental module (TEC1-12706) effective material properties.

Parameter	Value
Seebeck coefficient	$\alpha = 406.711\ \mu V/K$
Electrical resistivity	$\rho = 1.168 \times 10^{-3}\ \Omega{\cdot}cm$
TE thermal conductivity	$k = 0.058\ W/(cm{\cdot}K)$
Number of thermocouples	$n = 110$
The leg length of the TE element	$L_e = 1.35$ mm
The cross-sectional area of the TE element	$A_e = 1\ mm^2$
The dimensionless figure of merit at 298 K	$ZT = 0.726$

5. Conclusions

A TEG system for waste heat recovery from semi-truck automotive engines' exhaust was designed analytically and experimentally validated. The analytical design was formulated based on six energy-balance equations which covered enthalpy flow, convection heat transfer, and the ideal thermoelectric equations for the hot and cold junctions. The system was solved at steady state to determine the energy balance, as well as the junctions and ambient temperatures at the cold and hot sides of the system. Simultaneously, the load resistance and the number of couples of the TEG module were optimized until the maximum power output for one module reached 12.5 W. The heat sink was designed independently of the TEG module, and its fins' thickness and spacing were optimized to allow maximum exploitation of the waste heat flow. For the whole TEG system, 100 TEG modules were used. The total power output produced by the TEG system was 1.25 kW, representing 20% of the semi-truck engine's alternator power requirement, and a power density of 1.4 W/cm^2. Moreover, an experiment was conducted based on the commercially available TEG module in order to study the accuracy of the analytical model, where the measured junction temperatures and output power demonstrated good agreement with the theoretical results. Finally, the use of the effective material properties showed their significant influence on the improvement of the analytical design results' accuracy, as they incorporated the contact resistances and Thomson effect.

Author Contributions: Conceptualization, F.A.; methodology, F.A.; software, A.A.; validation, A.A.; formal analysis, A.A.; investigation, F.A.; resources, F.A.; data curation, A.A.; writing—original draft preparation, F.A.; writing—review and editing, F.A.; visualization, F.A.; supervision, A.A.; project administration, F.A. Both authors have read and agreed to the published version of the manuscript.

Funding: This research received no external funding.

Institutional Review Board Statement: Not applicable.

Informed Consent Statement: The authors acknowledge with thanks the Deanship of Scientific Research (DSR), at King Abdulaziz University, Jeddah, for technical and financial support. The authors also would like to thank Alwaleed Alshehri, Feras Maghrabi, and Moaaz Alsaigh for their help with this project especially with the experiment.

Data Availability Statement: The data presented in this study are available on request from the corresponding author. The data are not publicly available due to privacy.

Acknowledgments: The authors acknowledge with thanks the Deanship of Scientific Research.

Conflicts of Interest: The authors declare no conflict of interest.

References

1. Khan, M.; Subramaniyan, M.; Gurusamy, M. Power generation from waste heat of vehicle exhaust using thermo electric generator: A review. *IOP Conf. Ser. Mater. Sci. Eng.* **2018**, *402*, 12174. [CrossRef]
2. Fagehi, H. Optimal Design of Automotive Exhaust Thermoelectric Generator (AETEG). Master's Thesis, Westren Michigan University, Kalamazoo, MI, USA, 2016; p. 764.
3. Fagehi, H.; Attar, A.; Lee, H. Optimal Design of an Automotive Exhaust Thermoelectric Generator. *J. Electron. Mater.* **2018**, *47*, 3983–3995. [CrossRef]

4. Birkholz, U.; Grob, E.; Stohrer, U.; Voss, K.; Gruden, D.; Wurster, W. Conversion of Waste Exhaust Heat in Automobile using $FeSi_2$ Thermoelements. In Proceedings of the 7th International Conference on Thermoelectric Energy Conversion, Arlington, TX, USA, 16–18 March 1988; pp. 124–128.
5. Bass, J.C.; Elsner, N.B.; Leavitt, F.A. Performance of the 1 kW thermoelectric generator for diesel engines. *AIP Conf. Proc.* **1994**, *316*, 295–298.
6. Matsubara, K. Development of a high efficient thermoelectric stack for a waste exhaust heat recovery of vehicles. In Proceedings of the Twenty-First International Conference on Thermoelectrics, ICT '02, Long Beach, CA USA, 25–29 August 2002; pp. 418–423.
7. Jänsch, D. *Thermoelektrik Eine Chance für die Automobilindustrie*; Expert verlag GmbH: Tübingen, Germay, 2009.
8. Yang, J. Engineering and Materials for Automotive Thermoelectric Applications. In Proceedings of the 2009 Thermoelectrics Applications Workshop, San Diego, CA, USA, 29 September–2 October 2009; Available online: https://www.energy.gov/sites/prod/files/2014/03/f13/yang_0.pdf (accessed on 11 October 2020).
9. Salvador, J.R.; Cho, J.Y.; Ye, Z.; Moczygemba, J.E.; Thompson, A.J.; Sharp, J.W.; König, J.; Maloney, R.; Thompson, T.; Sakamoto, J.; et al. Thermal to Electrical Energy Conversion of Skutterudite-Based Thermoelectric Modules. *J. Electron. Mater.* **2013**, *42*, 1389–1399. [CrossRef]
10. Yu, C.; Chau, K. Thermoelectric automotive waste heat energy recovery using maximum power point tracking. *Energy Convers. Manag.* **2009**, *50*, 1506–1512. [CrossRef]
11. Liu, X.; Deng, Y.D.; Li, Z.; Su, C.Q. Performance analysis of a waste heat recovery thermoelectric generation system for automotive application. *Energy Convers. Manag.* **2015**, *90*, 121–127. [CrossRef]
12. Zhang, Y.; Cleary, M.; Wang, X.; Kempf, N.; Schoensee, L.; Yang, J.; Joshi, G.; Meda, L. High-temperature and high-power-density nanostructured thermoelectric generator for automotive waste heat recovery. *Energy Convers. Manag.* **2015**, *105*, 946–950. [CrossRef]
13. Kim, T.Y.; Negash, A.A.; Cho, G. Waste heat recovery of a diesel engine using a thermoelectric generator equipped with customized thermoelectric modules. *Energy Convers. Manag.* **2016**, *124*, 280–286. [CrossRef]
14. Li, X.; Xie, C.; Quan, S.; Shi, Y.; Tang, Z. Optimization of Thermoelectric Modules' Number and Distribution Pattern in an Automotive Exhaust Thermoelectric Generator. *IEEE Access* **2019**, *7*, 72143–72157. [CrossRef]
15. Li, G.; Zhu, D.; Zheng, Y.; Guo, W. Mesoscale combustor-powered thermoelectric generator with enhanced heat collection. *Energy Convers. Manag.* **2020**, *205*, 112403. [CrossRef]
16. Sivaprahasam, D.; Harish, S.; Gopalan, R.; Sundararajan, G. Automotive Waste Heat Recovery by Thermoelectric Generator Technology. In *Bringing Thermoelectricity into Reality*; Aranguren, P., Ed.; IntechOpen: London, UK, 2018.
17. Lee, H.S. *Thermoelectrics: Design and Materials*; John Wiley & Sons: Chichester, UK, 2017.
18. Lee, H. *Thermal Design Heat Sinks, Thermoelectrics, Heat Pipes, Compact heat Exchangers, and Solar Cells*; John Wiley & Sons: Hoboken, NJ, USA, 2010.
19. Weera, S.; Lee, H.; Attar, A. Utilizing effective material properties to validate the performance of thermoelectric cooler and generator modules. *Energy Convers. Manag.* **2020**, *205*, 112427. [CrossRef]
20. Kumar, S.; Heister, S.D.; Xu, X.; Salvador, J.R.; Meisner, G.P. Thermoelectric Generators for Automotive Waste Heat Recovery Systems Part I: Numerical Modeling and Baseline Model Analysis. *J. Electron. Mater.* **2013**, *42*, 665–674. [CrossRef]
21. Attar, A.; Lee, H.; Snyder, G.J. Optimum load resistance for a thermoelectric generator system. *Energy Convers. Manag.* **2020**, *226*, 113490. [CrossRef]